Hindawi
Journal of Chemistry
Volume 2019, Article ID 2428505, 10 pages
https://doi.org/10.1155/2019/2428505

Research Article

Adsorption of Bisphenol A on Peanut Shell Biochars: The Effects of Surfactants

Fang Wang[1], **Qiang Zeng**[1], **Wenting Su**[1], **Min Zhang**[1], **Lei Hou**[2] and **Zhong-Liang Wang**[1]

[1]*Tianjin Key Laboratory of Water Resources and Environment, Tianjin Normal University, Tianjin 300387, China*
[2]*College of Ecology and Environment, Southwest Forestry University, Kunming 650224, China*

Correspondence should be addressed to Lei Hou; leihou@swfu.edu.cn

Received 17 June 2019; Accepted 30 August 2019; Published 16 December 2019

Guest Editor: Peng Zhang

Bisphenol A (BPA) is a typical endocrine-disrupting chemical. The removal of BPA has raised much concerns in recent years. This paper examined the adsorption behavior of BPA to biochars and the different effects of cationic, anionic, and nonionic surfactants. The results indicated that peanut shell biochars prepared at 300°C (BC300), 500°C (BC500), and 700°C (BC700) showed strong adsorption affinity for BPA, and the adsorption affinity of biochars increased with the increase of pyrolysis temperature. The range of log K_d values was 2.83~3.71, 2.91~4.57, and 3.24~5.50 for BC300, BC500, and BC700, respectively. Both the type of surfactants and the properties of biochars could affect the adsorption behavior of BPA. Cetyltrimethyl ammonium bromide (CTAB) showed negligible effect on the adsorption of BPA on BC300, and the inhibition effect of CTAB was stronger with the increase of biochar pyrolysis temperature. Tween 20 and sodium dodecyl benzene sulfonate (SDBS) showed stronger inhibition effect than CTAB, especially on BC300. This is likely because the inhibition effect caused by competition of CTAB may be counterbalanced by the enhancement caused by the partitioning effect by adsorbed CTAB and the bridge effect between the $-NH_4^+$ group of CTAB and the phenol group on BPA/O-functional groups of biochars, whereas Tween 20 and SDBS do not have this bridge effect advantage. This study could provide insightful information for the application of biochars in removal of BPA.

1. Introduction

Bisphenol A (BPA) is one of the most common endocrine-disrupting chemicals, which is widely applied to produce plastics, resins, and other materials [1]. It could mimic or block the biological activity of natural hormones in the endocrine systems of wildlife and humans and may interfere with the transport and metabolic processes of natural hormones and threaten the health of wildlife and human even at trace levels (ng/L) [2, 3]. In recent years, BPA has been frequently detected in air, soil, sediments, water bodies, and food, and the concentration could reach as high as several milligram per liter [1, 4–6]. Therefore, it is of great importance to find an efficient method for BPA removal.

Biochar, which is a kind of carbon-rich, porous, and low-cost product formed by pyrolysis of biomass [7–9], has been reported to be an excellent adsorbent in wastewater treatment, especially for hydrophobic organic pollutants [10]. Previous studies found that biochars showed strong adsorption affinities to BPA [11–13]. For example, Wu et al. [11] have reported that wood, walnut, and apricot shell biochars all showed strong adsorption affinity to BPA. Choi et al. [12] showed that the maximum adsorption capacity of BPA to alfalfa biochar prepared at 650°C was as high as 38 mg/g. Kim et al. [13] reported that the adsorptive capacity of BPA to biochars is even stronger than that to powdered activated carbon. The adsorption behavior of biochars could be affected by aqueous chemistry conditions once they were applied in wastewater treatment [14, 15]. Surfactants, which are widely used in the daily life of humans, such as personal care products, textiles, pesticide formulations, pharmaceuticals, and household cleaning detergents [16], could be released into the environment and coexist with the organic contaminants. However, the influences of surfactants on the adsorption behavior of the organic contaminants to biochars were not fully investigated yet [17–19].

It is noted that there are many different types of surfactants, such as anionic surfactants, cationic surfactants, and nonionic surfactants. Therefore, they could have different effects on the adsorption behavior of organic contaminants due to their different chargeability and functional groups. For example, Zhang et al. [20] reported that high concentration of cationic surfactant, cetyltrimethyl ammonium bromide (CTAB), could enhance the adsorption of phenanthrene on black carbon, whereas high concentration of anionic surfactant, sodium dodecyl benzene sulfonate (SDBS), inhibited the adsorption of phenanthrene. This is likely because the phenanthrene molecular could be adsorbed on the hemimicelles or cosmids formed by CTAB which was adsorbed on black carbon and the adsorption was enhanced, whereas the presence of SDBS in the solution could increase the solubility of phenanthrene and inhibited the adsorption. On the contrary, Oleszczuk and Xing [21] reported that SDBS could enhance the dispersibility of the multiwalled carbon nanotubes, which led to the increase of oxytetracycline adsorption sites and strong enhancement of adsorption affinity to multiwalled carbon nanotubes, whereas the presence of TX100 and CTAB decreased the adsorption of oxytetracycline by multiwalled carbon nanotubes significantly. These studies indicated that the effects of surfactants on adsorption behavior were not only in relation to the types of the surfactants but also in relation to the properties of adsorbents. Up to now, there are few studies focused on the effects of different types of surfactants on the adsorption of BPA on biochars. Thus, it is of great importance to explore the effects of surfactants on the adsorption behavior of BPA to biochars and compare the differences between the different types of surfactants.

In this paper, the adsorption behavior of BPA to peanut shell biochars was examined, and the effects of different types of surfactants were also evaluated. CTAB, SDBS, and Tween 20 were selected as the model cationic, anionic, and nonionic surfactants, respectively. Physicochemical properties of peanut shell biochars under different pyrolysis temperatures were characterized. The adsorption affinities of BPA to the peanut shell biochars in absence and presence of the surfactants were examined by batch experiment. The controlling mechanisms were also discussed.

2. Materials and Methods

2.1. Chemicals. BPA was purchased from Sigma-Aldrich (Shanghai, China). The physicochemical properties are shown in Table 1. The three types of surfactants, CTAB, SDBS, and Tween 20, were all purchased from Sinopharm Chemical Reagent Co., Ltd. (Shanghai, China). Their critical micelle concentrations and molecular structures are summarized in Table 2. Methanol was purchased from Kangkede Technology Co., Ltd. (Tianjin, China). Disodium hydrogen phosphate (Na_2HPO_4) and sodium dihydrogen phosphate (NaH_2PO_4) were obtained from Guangfu Technology Development Co. Ltd. (Tianjin, China).

Table 1: Selected physicochemical properties of BPA.

Adsorbate	Molecular structure[a]	C_{sat} (mg/L)	Log K_{OW}	pK_a
Bisphenol A[a]	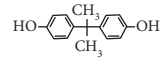	380	2.2	9.6

[a]From Pan et al. [22].

2.2. Biochar Preparation. Peanut shells were collected from Linyi (Shandong, China). Biochars were prepared as follows [25]. First, peanut shells were rinsed with distilled water. After air-drying, they were cut into small pieces and placed in a ceramic pot. The samples were then heated in a muffle furnace at 300, 500, and 700 °C for 2 h. Finally, the samples were grinded, and the biochar powders which passed through a 0.147 mm sieve were referred as BC300, BC500, and BC700, respectively.

2.3. Characterization of Biochars. Surface elemental compositions of the biochars were determined with X-ray photoelectron spectroscopy (XPS) (PHI 5000, VersaProbe, Japan). Fourier-transform infrared (FTIR) transmission spectra were obtained using a 110 Bruker Tensor 27 apparatus (Bruker Optics Inc., Germany), with a biochar to KBr ratio of 1 : 100. The morphological structures of the biochars were observed by both the scanning electron microscopy (SEM, S-3400N II, Hitachi, Japan) and transmission electron microscopy (TEM, JEM-2100, JEOL, Japan). The surface areas of the biochars were calculated using the multipoint Brunauer–Emmett–Teller method. The micropore volume and diameter were determined using the Horvath–Kawazoe method. The pH of point of zero charge (pH_{PZC}) of biochar was determined using the method reported by Dastgheib et al. [26].

2.4. Adsorption Experiments. The adsorption isotherm experiment of BPA on biochar was carried out by the batch experiment [12]. First, 10 mg of biochars was added to a glass vial, and then 20 mL of buffer solution (10 mM Na_2HPO_4-NaH_2PO_4, pH = 6.0) was spiked to the vial. When adsorption isotherm experiment in presence of surfactants was conducted, the surfactant solutions were added as the background solution and the surfactant concentration was set as 40 mg/L. Subsequently, certain amounts of BPA stock solution were added to the vials to make the initial concentration in the range of 0.44 to 28 mg/L. The volume of stock solution added to vials was kept below 0.1% to minimize the cosolvent effect. Then, the vials were tumbled at 3 rpm at room temperature for 14 days until the adsorption equilibrium was reached, and the concentrations of BPA in the supernatants were measured.

To test the effect of the concentration of surfactant, the concentrations of surfactant were set as 0.05, 0.1, 0.3, 0.5, and 0.8 CMC of each surfactant. The initial concentration of BPA was 4.5 mg/L. All the adsorption isotherm experiments were

Table 2: Molecular weight (MW), critical micelle concentration (CMC), and molecular structure of the surfactants.

Surfactant	MW (g/mol)	CMC (mg/L)	Molecular structure
Sodium dodecyl benzene sulfonate (SDBS)[a]	348.48	490	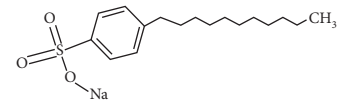
Cetyltrimethyl ammonium bromide (CTAB)[a]	1228	340	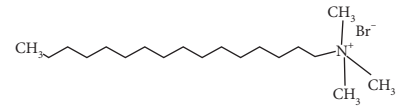
Tween 20, $n = \sim 20$[b]	1226	70	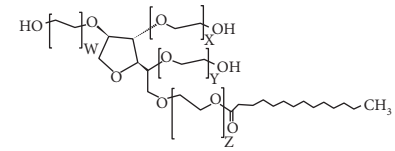

[a]From Han et al. [23]. [b]From Bak et al. [24].

run in duplicate, and the surfactant concentration effect experiments were run in triplicate.

2.5. Analytical Methods. The concentration of BPA was measured by a high-performance liquid chromatograph equipped with a 4.6 mm × 250 mm Eclipse Plus C18 column. The mobile phase was 70 : 30 (v/v) of methanol and deionized water with 1% acetic acid, and the flow rate was 1 mL/min. It was detected with a fluorescence detector at an excitation wavelength of 220 nm and an emission wavelength of 350 nm. No peaks were detected in the spectra for potential degraded/transformed products of the test compounds. All data were analyzed using Graph Pad Prism 6.

2.6. Statistical Analysis. One-way analysis of variance (ANOVA) with Duncan or Dunnett's T3 test was applied to test the significant differences of BPA solubility in presence and absence of surfactants and the effects of surfactant concentrations on the adsorption of BPA on BC300. Differences were considered significant at $p < 0.05$. All the statistical analyses were carried out using SPSS software (version 19.0, SPSS Inc., Chicago, USA).

3. Results and Discussion

3.1. Characterization of Biochars. The morphology properties of biochars can be described by SEM (Figure 1) and TEM images (Figure 2). It can be easily seen that the pore diameter of BC300 was 25.4 nm, which was significantly larger than that of BC500 and BC700, whereas the pore volume of BC300 was the smallest (Table 3). This was likely because during the pyrolysis of the biomass (i.e., peanut shell), it decomposed and a large number of fiber chain structures were destroyed [27]. Some substances under their volatilization temperature would deposit on the surface of the biochar and form an irregular block stack [27]. With the increase of pyrolysis temperature, the residual biomass was gradually decomposed, and the removal of volatile materials resulted in the increased pore volume [27–29].

The surface elemental compositions of biochars are summarized in Table 3. It was shown that with the increase of the pyrolysis temperature, the C content increased while N and O content decreased. Furthermore, (O + N)/C decreased from 0.29 to 0.23, which indicated the polarity of biochar decreased with the increasing pyrolysis temperature [28]. To further explore the changes in functional groups on the surface of different biochar samples, FTIR spectra are presented in Figure 3. The peaks around 3392, 1594, 1370, and 1030 cm^{-1} wavenumbers indicated the stretching vibration of O-H [30], double bond stretching vibration of C=O [31, 32], bending vibration of O-H [33], and stretching vibration of alkyl C-O [34] in the functional groups of biochars, respectively. The intensities of all these aforementioned peaks decreased with the increasing pyrolysis temperature. The content of each functional group was calculated based on XPS spectra. As shown in Figure 4 and Table 3, the content of C-C/C=C gradually increased with the increasing pyrolysis temperature, while that of oxygen-containing functional groups (e.g., C-O, C=O and COOH) decreased. This trend was consistent with the results of FTIR characterization. This is likely because with the increase of the pyrolysis temperature, the low degree of graphitized amorphous carbon could be converted to high degree of graphitized aromatic carbon via dehydration, decarboxylation, and decarbonylation effects [10, 32, 33, 35]. The loss of polar functional groups on the surface of biochar samples also resulted in the increase of pH_{PZC} value from 7.34 to 10.2 (Table 3) [36].

3.2. Adsorption of Bisphenol A by Biochar. The adsorption isotherms of BPA to BC300, BC500, and BC700 are shown in Figure 5. The adsorption data were fitted with the Freundlich sorption model: $q = K_F \cdot C_W^n$, where q (mg/kg) and

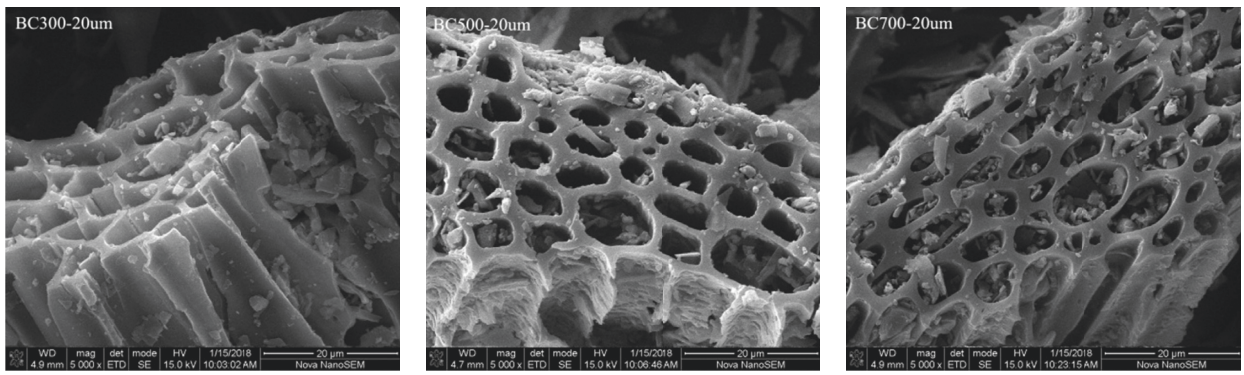

Figure 1: Scanning electron microscopy (SEM) images of BC300, BC500, and BC700.

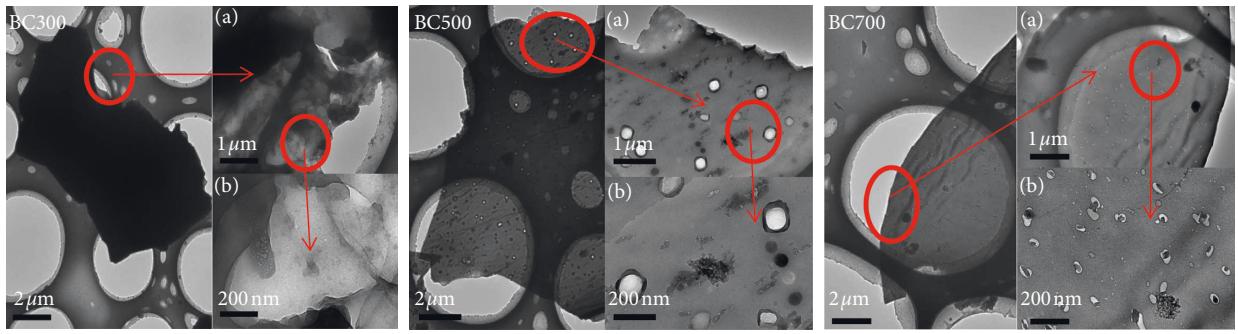

Figure 2: Transmission electron microscopy (TEM) images of BC300, BC500, and BC700 at different dimensions.

Table 3: Selected physicochemical properties of BC300, BC500, and BC700.

	C (wt%)[a]				Total C (wt.%)[a]	Total O (wt.%)[a]	Total N (wt.%)[a]	(O + N)/C ratio[a]	Specific surface area[b] ($m^2 \cdot g^{-1}$)	Pore volume[c] ($cm^3 \cdot g^{-1}$)	Pore diameter[c] (nm)	pH_{pzc}[d]
	C-C/C=C	C-O	C=O	COOH								
BC300	54.38	29.41	11.55	4.660	70.82	18.14	2.550	0.292	0.890	0.0058	25.4	7.34
BC500	68.68	16.23	10.80	4.300	73.33	16.56	2.250	0.256	58	0.053	3.66	9.93
BC700	74.00	11.66	10.32	4.030	75.02	14.81	2.150	0.226	376	0.23	2.32	10.2

[a]Analyzed using X-ray photoelectron spectroscopy. [b]Specific surface area measured using the Brunauer–Emmett–Teller (BET) method. [c]Volume of micropores (smaller than 20 Å in diameter) was determined using the Horvath–Kawazoe method. [d]Determined by a modified pH-drift method.

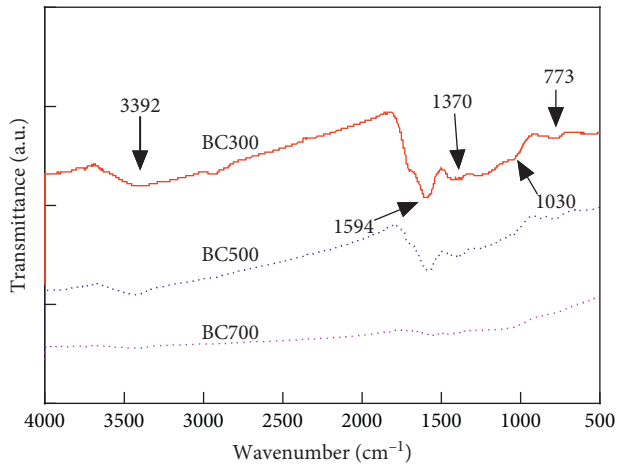

Figure 3: Fourier-transform infrared (FTIR) transmission spectra of BC300, BC500, and BC700.

C_W (mg/L) are the equilibrium concentrations of an adsorbate on the BCs and in the solution, respectively; K_F (mg^{1-n} L^n/kg) is the Freundlich affinity coefficient and n (unitless) is the Freundlich linearity index [37]. The n value could reflect the state of the energy distribution of the adsorption site [38, 39], and the heterogeneity of the adsorption sites increased with the decrease of n value [40]. The fitted Freundlich model parameters and the ranges of log K_d are summarized in Table 4, where K_d ($K_d = q/C_w$) is the adsorption coefficient [41]. In general, the Freundlich model fitted the adsorption data well.

As shown in Table 4, the values of n decreased from 0.48 to 0.22 with the increase of pyrolysis temperature. This is because the condensed aromatic domain of biochars and the heterogeneity of the adsorption sites increased with the increase of pyrolysis temperature [42]. The log K_d value of BC300 was in a range of 2.83~3.71, which was much lower than that of BC500 (2.91~4.57) and BC700 (3.24~5.50).

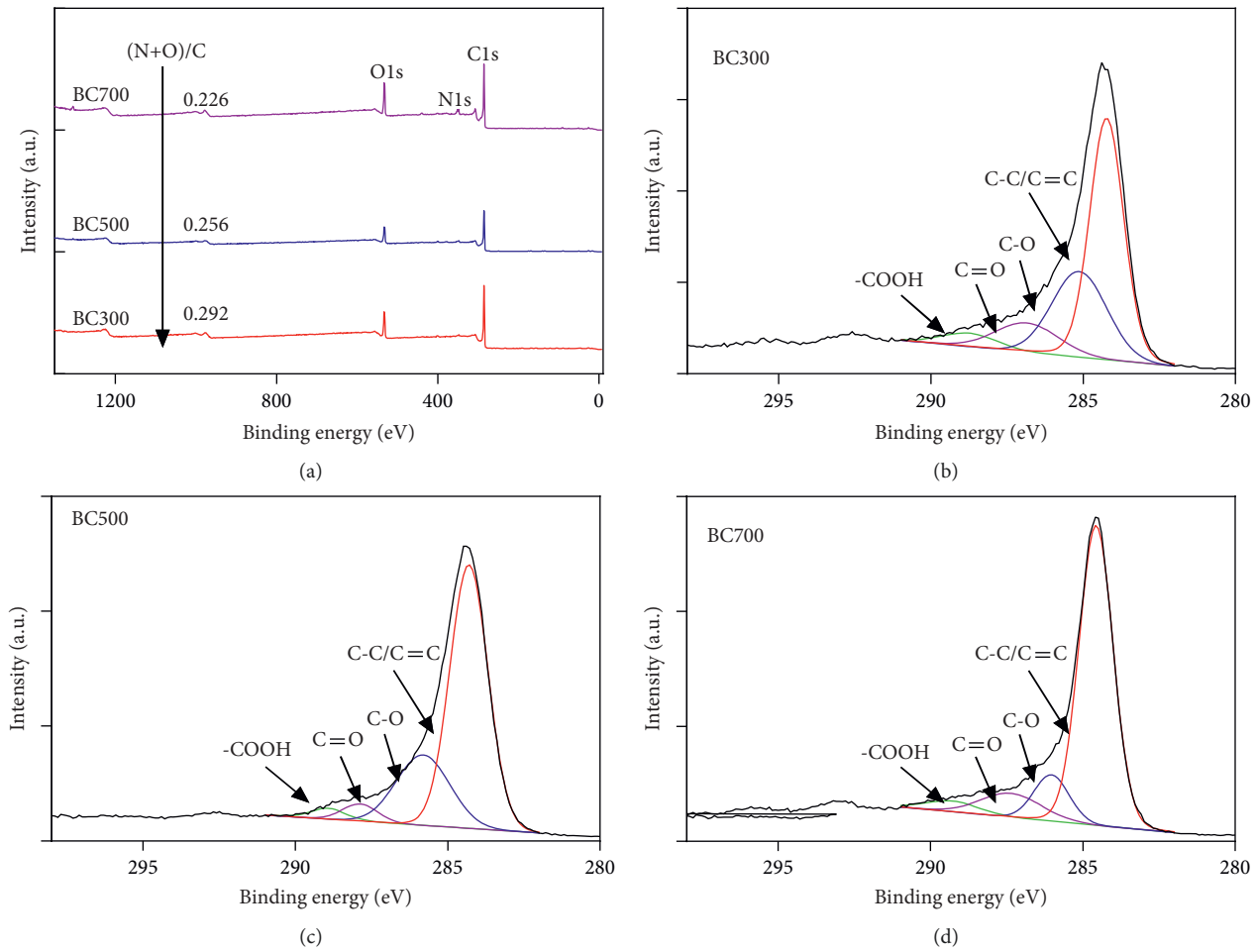

Figure 4: X-ray photoelectron spectroscopy (XPS) spectra and the C1s spectra of BC300, BC500, and BC700.

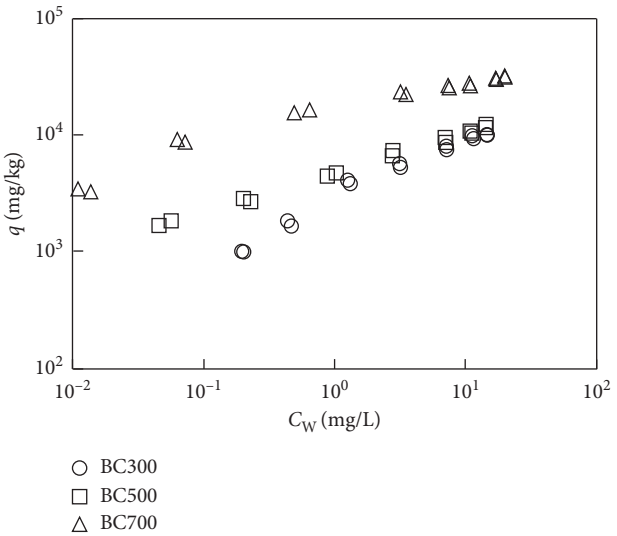

Figure 5: Adsorption isotherms of BPA to BC300, BC500, and BC700.

This result was comparable with the previous studies [11–13]. This also indicated that the adsorption affinity of biochars to BPA was following the order as BC700 > BC500 > BC300. One of the important reasons is that the increased pyrolysis temperature resulted in the enlarged pore volume and increased surface areas of biochar and provided more adsorption sites for BPA. On the other hand, the hydrophobicity of the biochar increased with the increase of pyrolysis temperature. Previous studies have reported that hydrophobic interaction is the main adsorption mechanism for the hydrophobic organic contaminants to biochars [27]. Therefore, the hydrophobic interaction between biochar and BPA was also enhanced. Thirdly, the amount of aromatic benzene ring of the biochar increased with the increase of pyrolysis temperature and made the biochars become a stronger π-electron acceptor. BPA could act as a strong a π-electron donor. Thus, the π-π electron donor/acceptor (EDA) interaction between biochar and BPA was enhanced. Chen et al. [27] also reported that π-π EDA interaction was one of the important factors that could affect the adsorption of BPA, which was consistent with our conclusion. It is noted that with the increase concentration of BPA, the adsorption affinity on the biochar under low pyrolysis temperature was closer to that on the biochar under high pyrolysis temperature. This is likely because biochars derived under low pyrolysis temperature contained more O-functional groups, and the H-bonding effect between the –OH group of BPA and the O-functional

Table 4: Summary of adsorption parameters (Freundlich model coefficients (K_F and n) and distribution coefficients (K_d)) obtained from adsorption results.

Adsorbent	Background	K_F (mmol^{1-n}L^n/kg)[a]	n[a]	R^2	Log K_d (L/kg)
BC300	None	3100 ± 170	0.45 ± 0.02	0.984	2.83–3.71
	CTAB	2200 ± 110	0.57 ± 0.02	0.993	2.75–3.68
	SDBS	1200 ± 88	0.35 ± 0.03	0.938	2.30–3.33
	Tween 20	1000 ± 70	0.43 ± 0.03	0.967	2.31–3.21
BC500	None	4700 ± 140	0.34 ± 0.01	0.992	2.91–4.57
	CTAB	3400 ± 230	0.54 ± 0.03	0.985	2.93–3.57
	SDBS	1800 ± 90	0.42 ± 0.02	0.980	2.57–3.49
	Tween 20	1700 ± 90	0.31 ± 0.02	0.960	2.42–3.55
BC700	None	16000 ± 520	0.22 ± 0.01	0.980	3.24–5.50
	CTAB	3200 ± 290	0.44 ± 0.04	0.965	3.77–4.49
	SDBS	4400 ± 280	0.33 ± 0.03	0.960	2.72–4.28
	Tween 20	5700 ± 240	0.31 ± 0.02	0.981	2.83–4.58

[a]Values after ± sign indicate relative standard deviation.

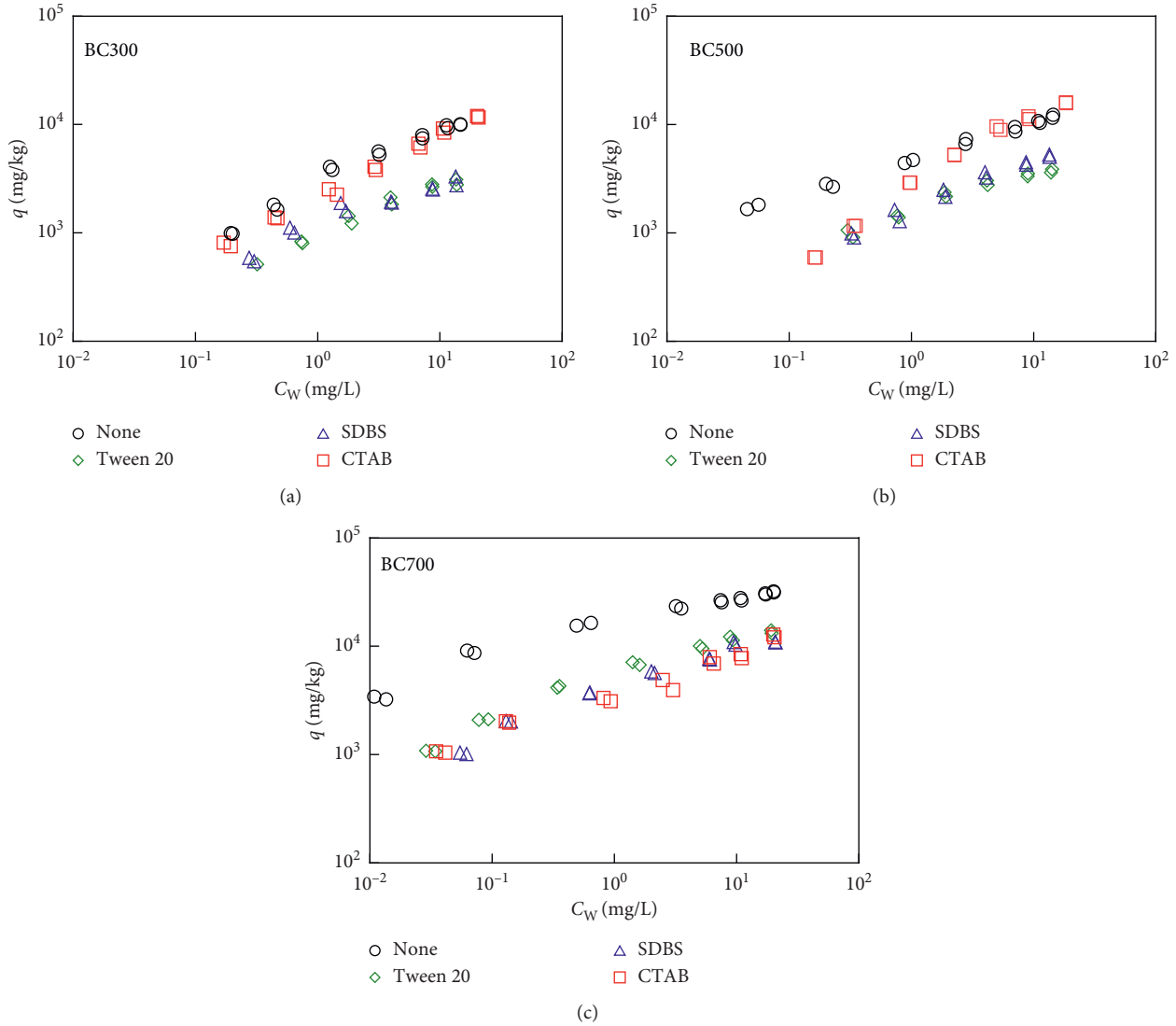

Figure 6: Adsorption isotherms of BPA to BC300, BC500, and BC700 in absence and presence of the surfactants.

groups on biochars was stronger [43]. With the increased concentration of BPA, the H-bonding effect was more obvious. Thus, although the hydrophobicity effect and π-π EDA interaction were weak on biochars derived under low pyrolysis temperature, the relatively stronger H-bonding, especially at higher BPA concentration, could offset part of the

hydrophobicity effect and π-π EDA interaction effect. Thus, H-bonding is another important mechanism that controls the adsorption behavior.

3.3. Adsorption of Bisphenol A by Biochar in presence of the Surfactants. The adsorption isotherms of BPA in presence of the surfactants are shown in Figure 6, and the fitted Freundlich model parameters are summarized in Table 4. The three different types of surfactants all showed inhibition effect on the adsorption of BPA. However, the extents of the inhibition varied, which may be in relation to the types of surfactants and the properties of biochars.

Previous studies have reported that the surfactants could be adsorbed on biochars via the hydrophobic effect, electrostatic attraction, cation exchange, π-π interaction, pore-filling effect, etc. [23, 44]. Thus, they could occupy the adsorption sites of the organic contaminants or block the pores that the organic contaminants may enter in [37]. On the other hand, the adsorbed surfactants on biochars could form hemimicelles or admicelles, which could also offer absorption (partitioning) sites for the organic contaminants [45]. Next, the surfactants could increase the solubility of organic contaminants [20]. Thus, the effects of the surfactants on the adsorption of organic contaminants depend on the contribution of each mechanism. To further explore the mechanisms that surfactants affect the adsorption behavior of BPA on biochars, the adsorption coefficient ($\log K_d$) of BPA in absence and presence of the surfactants at different equilibrium concentrations of BPA was calculated based on the Freundlich model (Table 5).

As shown in Figure 6, the adsorption isotherms of BPA on BC300 in presence of CTAB almost overlapped with that in absence of the surfactant. The $\log K_d$ varied less than 1.4% when the equilibrium concentration of BPA was 10 mg/L compared with that in absence of the surfactant on BC300, whereas it decreased 14.5% on BC700 (Table 5). Zhang et al. [20] reported that the solubilization effect could be an important reason that resulted in the inhibition effect in presence of surfactants. However, in our study, the experimental concentration of CTAB was 40 mg/L, which was much lower than the critical micelle concentration (CMC) of CTAB (340 mg/L). Thus, it has little effect on the solubility of BPA (Figure 7). Therefore, the solubility enhancement effect could be negligible. As shown in Table 2, the cationic CTAB molecules have a long hydrophobic chain and a positively charged "head" ($-NH_4^+$); thus, it could be adsorbed on the hydrophobic surface of biochars via the hydrophobic effect and the negatively charged O-functional groups via electrostatic attraction. As discussed earlier, these adsorption sites on the surface of biochars were also available for BPA. Thus, the adsorption sites for BPA would decrease in presence of CTAB, and the micropores of biochars that BPA could go in may be blocked. On the other hand, the partitioning of BPA to hemimicelles that adsorbed CTAB formed on BC300 could enhance the adsorption of BPA. Another important mechanism is that the $-NH_4^+$ group of CTAB could interact with the phenol group of BPA via Lewis acid-base interaction [37]. Thus, CTAB could serve as a cation bridge between the BPA and biochars and enhance the adsorption. Therefore, the adsorption isotherms of BPA in presence of CTAB almost overlapped with that in absence of surfactants probably due to the counterbalance between the inhibition effect caused by competition and the enhancement effect caused by the partitioning and the bridging effect by adsorbed CTAB.

It is noted that the inhibition effect of CTAB decreased with the increase of BPA concentration. For example, the adsorption coefficient ($\log K_d$) of BPA decreased 6.8% on BC300 at $C_W = 0.1$ mg/L compared with that in absence of CTAB, whereas it decreased 1.3% at $C_W = 10$ mg/L. At low concentration of BPA, the BPA molecules were prone to be adsorbed on the high adsorption energy sites, such as micropores. With the increase of the concentration of BPA, they started to be adsorbed on other adsorption sites with relatively low adsorption energy, such as the hemimicelles formed on biochars and NH_4^+ group of CTAB. Thus, the inhibition effect was weakened.

Tween 20 and SDBS showed similar inhibition effect on the BPA adsorption, which were different from CTAB, especially on BC300 (Figure 6). The $\log K_d$ values of BPA in

Table 5: The adsorption coefficients ($\log (K_d)$) calculated based on Freundlich model in absence and presence of the surfactants at different equilibrium concentrations of BPA.

Adsorbent	Background	Log K_d (L/kg)	
		$C_W = 0.1$ mg/L	$C_W = 10$ mg/L
BC300	None	4.05	2.94
	CTAB	3.77	2.90
	SDBS	3.75	2.44
	Tween 20	3.59	2.44
BC500	None	4.33	3.02
	CTAB	3.99	3.07
	SDBS	3.82	2.68
	Tween 20	3.91	2.55
BC700	None	4.99	3.44
	CTAB	4.07	2.94
	SDBS	4.31	2.97
	Tween 20	4.44	3.07

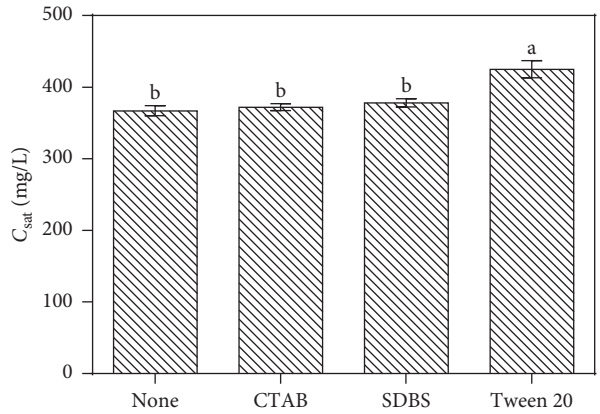

Figure 7: Solubility of BPA in absence and presence of the surfactants. The bars indicate the standard error of triplicates, and different letters indicate significant difference ($p < 0.05$).

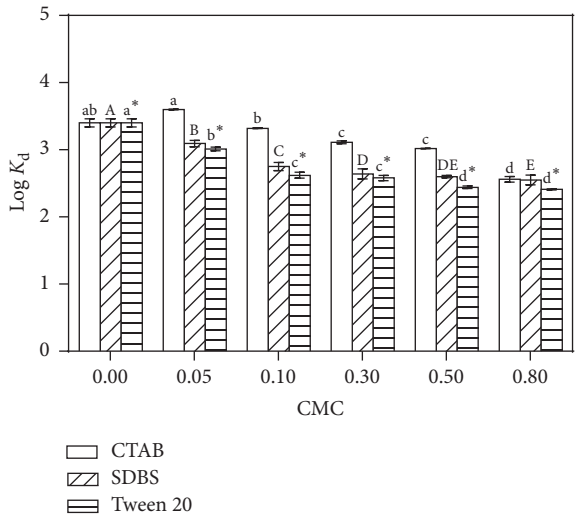

Figure 8: Effects of the surfactants on adsorption of BPA on BC300 under different surfactant concentrations. The bars indicate the standard error of triplicates, and different letters indicate significant difference ($p < 0.05$).

presence of SDBS and Tween 20 were 2.44, which was much lower than that in presence of CTAB (2.90). One of the important reasons is that Tween 20 and SDBS do not have the advantage of the bridging effect which is caused by the $-NH_4^+$ group of CTAB. Secondly, as shown in Figure 7, the solubility of BPA was increased by 15% in presence of Tween 20; thus, the BPA molecule was prone to dissolve in the surfactant solutions rather than being adsorbed on biochars [37]. On the other hand, Tween 20 could be adsorbed on the biochars via hydrophobic interaction due to its long hydrophobic chains structure, and the adsorption kinetics of Tween 20 was reported to be faster than that of BPA [46, 47]. Therefore, the molecules of Tween 20 could preferentially occupy the adsorption sites. Tween 20 could twine around the surface of biochars or block the entrances of micropores [46], and the available adsorption sites decreased. Thus, it inhibited the adsorption of BPA. Although SDBS was negatively charged and showed less adsorption on biochar surface [37], the hemimicelles or admicelles formed on biochar surface also decreased. According to the adsorption results, we speculated that the enhancement caused by the partitioning effect by adsorbed SDBS could not counterbalance the inhibition effect caused by competition effect. Thus, the inhibition effect was also strong in presence of SDBS.

With the increase of pyrolysis temperature, the extent of inhibition effect, which is indicated by the decreased percent of adsorption coefficient ($\log K_d$) (Table 5), was stronger in presence of CTAB, especially at low concentration of BPA. In presence of SDBS and Tween 20, the decreased percent of adsorption coefficient decreased less than that in presence of CTAB at low concentration of BPA, and it showed even a little increase at high concentration of BPA. This is likely because the pore diameter of biochars decreased with the increase of pyrolysis temperature. The adsorbed surfactant molecules could block more micropores on biochars produced at high pyrolysis temperature, and the inhibition effect of CTAB was stronger with the increase of pyrolysis temperature at low concentration of BPA. However, this may be not the main mechanism because of the different effects on CTAB and SDBS/Tween 20. With the increase of pyrolysis temperature, the O-functional groups of biochars decreased, and the zeta potential also decreased. Thus, the electronic attraction between CTAB and biochar decreased, and the adsorption of CTAB on biochars weakened. The enhancement caused by the partitioning effect by adsorbed CTAB and the bridging effect could not counterbalance the competition effect; thus, the inhibition effect became stronger.

To further identify the mechanisms controlling the effects of the surfactants, we examined the values of $\log K_d$ of BPA on BC300 under different surfactant concentrations (Figure 8). For SDBS and Tween 20, it showed similar trend that with the increase of the surfactant concentration, the inhibition effect was enhanced significantly ($p < 0.05$). This may be because with the increase of the surfactant concentration, the solubility enhancement effect also increased which may decrease the adsorption of BPA on biochars. Zhang et al. [20] also reported that the increase of SDBS concentration could result in decrease of phenanthrene adsorption on black carbon because of the solubility enhancement. However, CTAB showed a slight increase of BPA adsorption on biochars at lower concentration (0.05 CMC) ($p > 0.05$) and then decreased significantly ($p < 0.05$). This is likely because the partitioning effect and the bridging effect caused by adsorbed CTAB might be the main mechanisms at low concentration of CTAB.

4. Conclusion

The pyrolysis temperature could affect the physical and chemical properties of peanut shell biochar, and the adsorption affinity of BPA would be stronger on the biochars produced at higher temperature due to the larger surface area and pore volume, higher hydrophobicity, and aromaticity. The main mechanisms of adsorption of BPA on peanut shell biochars were hydrophobic effect, π-π EDA interaction, and H-bonding. The presence of surfactants could affect the adsorption behavior of BPA to biochars. The cationic, anionic, and nonionic surfactants all showed inhibition effect on the adsorption of BPA. The adsorption affinities of BPA in presence of CTAB were similar with those in absence of surfactants to BC300 probably due to the counterbalance between the inhibition effect caused by competition and enhancement caused by the partitioning and bridging effect by adsorbed CTAB, and the inhibition effect of CTAB was stronger with the increase of pyrolysis temperature. However, Tween 20 and SDBS do not have the advantage of the bridging effect which is caused by the $-NH_4^+$ group of CTAB. Thus, Tween 20 and SDBS showed stronger inhibition effect than CTAB, especially on BC300. This study revealed the mechanisms controlling the adsorption behavior of BPA to biochars. It is of great importance for the application of the biochar in wastewater treatment. However, further studies (in particular, the

desorption behavior in presence of surfactants) are needed to fully understand the mechanism of the adsorption process of BPA to biochars.

Data Availability

The data used to support the findings of this study are available from the corresponding author upon request.

Conflicts of Interest

The authors declare that there are no conflicts of interest regarding the publication of this paper.

Acknowledgments

This study was supported by the National Natural Science Foundation of China (grant nos. 21707101 and 21607120), Science and Technology Development Foundation of Tianjin Municipal Education Commission of China (grant no. JW1715), the Opening Foundation of Ministry of Education Key Laboratory of Pollution Processes and Environmental Criteria (grant no. 2017-06), the Doctoral Fund of Tianjin Normal University (grant no. 52XB1403), and the Innovation Team Training Plan of the Tianjin Education Committee (TD13-5073).

References

[1] Y. H. Ou, Y. J. Chang, F. Y. Lin, M. L. Chang, C. Y. Yang, and Y. H. Shih, "Competitive sorption of bisphenol A and phenol in soils and the contribution of black carbon," *Ecological Engineering*, vol. 92, pp. 270–276, 2016.

[2] A. Tomza-Marciniak, P. Stepkowska, J. Kuba, and B. Pilarczyk, "Effect of bisphenol A on reproductive processes: a review of in vitro, in vivo and epidemiological studies," *Journal of Applied Toxicology*, vol. 38, no. 1, pp. 51–80, 2018.

[3] K. Anongporn, P. Wachirasek, C. Nipon, and W. Orawan, "Damaging effects of bisphenol A on the kidney and the protection by melatonin: emerging evidences from in vivo and in vitro studies," *Oxidative Medicine and Cellular Longevity*, vol. 2018, Article ID 3082438, 15 pages, 2018.

[4] S. Flint, T. Markle, S. Thompson, and E. Wallace, "Bisphenol A exposure, effects, and policy: a wildlife perspective," *Journal of Environmental Management*, vol. 104, no. 16, pp. 19–34, 2012.

[5] Y. Q. Huang, C. K. C. Wong, J. S. Zheng et al., "Bisphenol A (BPA) in China: a review of sources, environmental levels, and potential human health impacts," *Environment International*, vol. 42, pp. 91–99, 2012.

[6] T. Yamamoto, A. Yasuhara, H. Shiraishi, and O. Nakasugi, "Bisphenol A in hazardous waste landfill leachates," *Chemosphere*, vol. 42, no. 4, pp. 415–418, 2001.

[7] L. Lu and B. Chen, "Enhanced bisphenol A removal from stormwater in biochar-amended biofilters: combined with batch sorption and fixed-bed column studies," *Environmental Pollution*, vol. 243, pp. 1539–1549, 2018.

[8] P. Zhang, H. Sun, L. Yu, and T. Sun, "Adsorption and catalytic hydrolysis of carbaryl and atrazine on pig manure-derived biochars: impact of structural properties of biochars," *Journal of Hazardous Materials*, vol. 244-245, pp. 217–224, 2013.

[9] P. Zhang, G. Huang, C. An et al., "An integrated gravity-driven ecological bed for wastewater treatment in subtropical regions: process design, performance analysis, and greenhouse gas emissions assessment," *Journal of Cleaner Production*, vol. 212, pp. 1143–1153, 2019.

[10] A. Ghaffar, S. Ghosh, F. Li et al., "Effect of biochar aging on surface characteristics and adsorption behavior of dialkyl phthalates," *Environmental Pollution*, vol. 206, pp. 502–509, 2015.

[11] Z. Wu, X. Wei, Y. Xue, X. He, and X. Yang, "Removal effect of atrazine in co-solution with bisphenol A or humic acid by different activated carbons," *Materials*, vol. 11, no. 12, p. 2558, 2018.

[12] Y. K. Choi and E. Kan, "Effects of pyrolysis temperature on the physicochemical properties of alfalfa-derived biochar for the adsorption of bisphenol A and sulfamethoxazole in water," *Chemosphere*, vol. 218, pp. 741–748, 2019.

[13] E. Kim, C. Jung, J. Han et al., "Sorptive removal of selected emerging contaminants using biochar in aqueous solution," *Journal of Industrial and Engineering Chemistry*, vol. 36, pp. 364–371, 2016.

[14] J. Chen, D. Zhu, and C. Sun, "Effect of heavy metals on the sorption of hydrophobic organic compounds to wood charcoal," *Environmental Science and Technology*, vol. 41, no. 7, pp. 2536–2541, 2007.

[15] B. Sun, F. Lian, Q. Bao, Z. Liu, Z. Song, and L. Zhu, "Impact of low molecular weight organic acids (lmwoas) on biochar micropores and sorption properties for sulfamethoxazole," *Environmental Pollution*, vol. 214, pp. 142–148, 2016.

[16] G.-G. Ying, "Fate, behavior and effects of surfactants and their degradation products in the environment," *Environment International*, vol. 32, no. 3, pp. 417–431, 2006.

[17] W. Que, L. Jiang, C. Wang et al., "Influence of sodium dodecyl sulfate coating on adsorption of methylene blue by biochar from aqueous solution," *Journal of Environmental Sciences*, vol. 70, no. 8, pp. 166–174, 2018.

[18] X. Mi, G. Li, W. Zhu, and L. Liu, "Enhanced adsorption of orange II using cationic surfactant modified biochar pyrolyzed from cornstalk," *Journal of Chemistry*, vol. 2016, Article ID 8457030, 7 pages, 2016.

[19] D. Han, X. T. Liu, G. X. Zhang, K. Sun, and Y. Jiao, "Effects of cationic surfactant on pentachlorophenol sorption by sediment activecarbon and biochar," *Fresenius Environmental Bulletin*, vol. 22, no. 4B, pp. 1280–1286, 2013.

[20] J. Zhang and M. He, "Effect of surfactants on sorption and desorption of phenanthrene onto black carbon," *Water Environment Research*, vol. 83, no. 1, pp. 15–22, 2011.

[21] P. Oleszczuk and B. Xing, "Influence of anionic, cationic and nonionic surfactants on adsorption and desorption of oxytetracycline by ultrasonically treated and non-treated multiwalled carbon nanotubes," *Chemosphere*, vol. 85, no. 8, pp. 1312–1317, 2011.

[22] B. Pan, D. Lin, H. Mashayekhi, and B. Xing, "Adsorption and hysteresis of bisphenol A and 17α-ethinyl estradiol on carbon nanomaterials," *Environmental Science and Technology*, vol. 43, no. 2, pp. 5480–5485, 2008.

[23] Z. Han, F. Zhang, D. Lin, and B. Xing, "Clay minerals affect the stability of surfactant-facilitated carbon nanotube suspensions," *Environmental Science and Technology*, vol. 42, no. 18, pp. 6869–6875, 2008.

[24] A. Bak and W. Podgórska, "Interfacial and surface tensions of toluene/water and air/water systems with nonionic surfactants Tween 20 and Tween 80," *Colloids and Surfaces A: Physicochemical Engineering Aspects*, vol. 504, pp. 414–425, 2016.

[25] J. Li, N. Liang, X. Jin et al., "The role of ash content on bisphenol A sorption to biochars derived from different agricultural wastes," *Chemosphere*, vol. 171, pp. 66–73, 2017.

[26] S. A. Dastgheib, T. Karanfil, and W. Cheng, "Tailoring activated carbons for enhanced removal of natural organic matter from natural waters," *Carbon*, vol. 42, no. 3, pp. 547–557, 2004.

[27] J. Chen, D. Zhang, H. Zhang, S. Ghosh, and B. Pan, "Fast and slow adsorption of carbamazepine on biochar as affected by carbon structure and mineral composition," *Science of the Total Environment*, vol. 579, pp. 598–605, 2016.

[28] Z. Chen, B. Chen, and C. T. Chiou, "Fast and slow rates of naphtalene sorption to biochars produced at different temperatures," *Environmental Science and Technology*, vol. 46, no. 20, pp. 11104–11111, 2012.

[29] H. Zheng, Z. Wang, J. Zhao, S. Herbert, and B. Xing, "Sorption of antibiotic sulfamethoxazole varies with biochars produced at different temperatures," *Environmental Pollution*, vol. 181, pp. 60–67, 2013.

[30] Y. Fu, N. Zhang, Y. Shen, X. Ge, and M. Chen, "Micro-mesoporous carbons from original and pelletized rice husk via one-step catalytic pyrolysis," *Bioresource Technology*, vol. 269, pp. 67–73, 2018.

[31] G. Chu, J. Zhao, F. Chen et al., "Physi-chemical and sorption properties of biochars prepared from peanut shell using thermal pyrolysis and microwave irradiation," *Environmental Pollution*, vol. 227, pp. 372–379, 2017.

[32] M. Ahmad, S. S. Lee, X. Dou et al., "Effects of pyrolysis temperature on soybean stover- and peanut shell-derived biochar properties and TCE adsorption in water," *Bioresource Technology*, vol. 118, pp. 536–544, 2012.

[33] M. Keiluweit, P. S. Nico, M. G. Johnson, and M. Kleber, "Dynamic molecular structure of plant biomass-derived black carbon (biochar)," *Environmental Science and Technology*, vol. 44, no. 4, pp. 1247–1253, 2010.

[34] M. Lawrinenko, D. Jing, C. Banik, and D. A. Laird, "Aluminum and iron biomass pretreatment impacts on biochar anion exchange capacity," *Carbon*, vol. 118, pp. 422–430, 2017.

[35] Z. Chang, L. Tian, M. Wu, X. Dong, J. Peng, and B. Pan, "Molecular markers of benzene polycarboxylic acids in describing biochar physiochemical properties and sorption characteristics," *Environmental Pollution*, vol. 237, pp. 541–548, 2018.

[36] L. Ye, J. Zhang, J. Zhao, Z. Luo, S. Tu, and Y. Yin, "Properties of biochar obtained from pyrolysis of bamboo shoot shell," *Journal of Analytical and Applied Pyrolysis*, vol. 114, pp. 172–178, 2015.

[37] F. Wang, Z. Jia, W. Su, Y. Shang, and Z.-L. Wang, "Adsorption of phenanthrene and 1-naphthol to graphene oxide and L-ascorbic-acid-reduced graphene oxide: effects of pH and surfactants," *Environmental Science and Pollution Research*, vol. 26, no. 11, pp. 11062–11073, 2019.

[38] N. Xu, B. Zhang, G. Tan, J. Li, and H. Wang, "Influence of biochar on sorption, leaching and dissipation of bisphenol A and 17α-ethynylestradiol in soil," *Environmental Science: Processes and Impacts*, vol. 17, no. 10, pp. 1722–1730, 2015.

[39] M. Wu, B. Pan, D. Zhang et al., "The sorption of organic contaminants on biochars derived from sediments with high organic carbon content," *Chemosphere*, vol. 90, no. 2, pp. 782–788, 2013.

[40] H. Li, C. Wei, D. Zhang, and B. Pan, "Adsorption of bisphenol A on dispersed carbon nanotubes: role of different dispersing agents," *Science of the Total Environment*, vol. 655, pp. 807–813, 2019.

[41] C. Jung, J. Park, K. H. Lim et al., "Adsorption of selected endocrine disrupting compounds and pharmaceuticals on activated biochars," *Journal of Hazardous Materials*, vol. 263, pp. 702–710, 2013.

[42] K. Sun, K. Ro, M. Guo, J. Novak, H. Mashayekhi, and B. Xing, "Sorption of bisphenol A, 17α-ethinyl estradiol and phenanthrene on thermally and hydrothermally produced biochars," *Bioresource Technology*, vol. 102, no. 10, pp. 5757–5763, 2011.

[43] P. Wu, Z. Cai, H. Jin, and Y. Tang, "Adsorption mechanisms of five bisphenol analogues on pvc microplastics," *Science of the Total Environment*, vol. 650, pp. 671–678, 2019.

[44] Q. Wang, Y. Han, Y. Wang, Y. Qin, and Z.-X. Guo, "Effect of surfactant structure on the stability of carbon nanotubes in aqueous solution," *The Journal of Physical Chemistry B*, vol. 112, no. 24, pp. 7227–7233, 2008.

[45] K. Yang, Q. Jing, W. Wu, L. Zhu, and B. Xing, "Adsorption and conformation of a cationic surfactant on single-walled carbon nanotubes and their influence on naphthalene sorption," *Environmental Science and Technology*, vol. 44, no. 2, pp. 681–687, 2010.

[46] C. K. Ahn, S. H. Woo, and J. M. Park, "Enhanced sorption of phenanthrene on activated carbon in surfactant solution," *Carbon*, vol. 46, no. 11, pp. 1401–1410, 2008.

[47] C. K. Ahn, Y. M. Kim, S. H. Woo, and J. M. Park, "Selective adsorption of phenanthrene dissolved in surfactant solution using activated carbon," *Chemosphere*, vol. 69, no. 11, pp. 1681–1688, 2007.